

# Application of the Folding-Averaging Algorithm for the Determination of the Periods of the Earth's Free Oscillation Using Superconducting Gravimeter Data

J. Y. Guo<sup>a,b</sup>, H. Greiner-Mai<sup>b</sup>, O. Dierks<sup>b</sup>, L. Ballani<sup>b</sup>, J. Neumeyer<sup>b</sup>, C. K. Shum<sup>c</sup>

<sup>a</sup>The Key Laboratory of Geospace Environment and Geodesy, Ministry of Education, School of Geodesy and Geomatics, Wuhan University, 129 Luoyu Road, 430079 Wuhan, China. Email: junyiguo@public.wh.hb.cn

<sup>b</sup>GeoForschungsZentrum Potsdam, Section 1.3, Telegrafenberg A17, D-14473 Potsdam, Germany

<sup>c</sup>Laboratory for Space Geodesy and Remote Sensing, The Ohio State University, 2070 Neil Avenue, Columbus, Ohio 43210-1275, USA

## Abstract

A stacking method, which is referred as folding-averaging algorithm (FAA) in this paper, was frequently used for evaluating discrete Fourier transform (DFT) before the fast Fourier transform (FFT) technique was conceived. In this paper, we reformulate the FAA to precisely determine periods of signals which may be present in a time series. The basic principle of the FAA is to rebuild for every test period a new short time series by cutting the original time series to shorter ones of which the length is equal to the test period (at the end of the time series, a small fraction shorter than the test period may be discarded), and then stacking the short time series by averaging. In this stacking process of averaging, the amplitude of the possible signal with a period equal to the test period remains the same, but signals of different periods are averaged out and the random error is reduced. Amplitude and phase of the possible signal with a period equal to the test period can then be estimated using the averaged short time series. By searching for the maximum extremes of the amplitude by varying the test period, the periods of the signals which may be present in the time series can be very precisely determined. The FAA is distinct from DFT as follows: in FAA, periods of possible real physical signals in the time series are sought; but in DFT, sinusoidal functions with prescribed periods which are submultiples of the length of the time series are used to represent the time series exactly. The usefulness of the FAA is illustrated by applying it to determine the periods of the Earth's free oscillations using superconducting gravimeter (SG) data after the Peruvian Earthquake of magnitude 8.4 in 2001.

*keywords:* Time series; Folding-averaging algorithm; Period determination; Earth's free oscillation; superconducting gravimeter observation

## 1 Introduction

Retrieving periodical signals buried in a time series has been a topics heavily investigated in many branches of science, notably geophysics. Undoubtedly, the most well known method used nowadays in time series analysis is the DFT, or called FFT as a fast evaluation version. Having an inverse transform, the DFT gives exact representations of a time series using sinusoidal functions of which the periods are submultiples of the length of the time series. But in real physical problems, the period of a signal depends on its physical cause other than the length of observation, and hence, is not necessarily equal to a certain submultiple of the length of the time series obtained from observation. From this point of view, the DFT is not really relevant in determining periods of real physical signals in time series. A remedy to this weakness is to fit the Fourier spectrum around a peak with a resonance function (Bolt and Brillinger, 1979; Dahlen, 1982; Masters and Gilbert, 1983).

Unlike DFT, as can be seen from the process of constructing the averaged short time series stated in the abstract, the FAA is designed for searching for periods of real physical signals in time series other than giving exact representations of time series using prescribed periodical functions. For example, assume that a sinusoidal signal with a period of 0.985 hour is present in a time series of 100 hours. When using DFT to analyze this time series, the periods of sinusoidal waves we obtain nearest to 0.985 are  $100/102 \approx 0.98$  and  $100/101 \approx 0.99$ . But when using the FAA for searching for periods of signals, a test period may be chosen as close to 0.985 as possible by increasing the density of test periods in the search. The precision of the period finally found depends on the sampling interval as well as the error of observation. Problems of precision will be discussed in the next section together with the FAA it self. Here we only point out that, if there is only one sinusoidal signal in a time series and there is no observation error, the precision of the period obtained for the signal is about  $2(T/L_{TS})\Delta t$ , where  $T$  is the period of the sinusoidal wave,  $L_{TS}$  is the length of the time series, and  $\Delta t$  is the sampling interval. For the above numerical example, if the sampling

interval is 0.1 hour, the precision of the period obtained according to this criteria should be about 0.002 hour that is more accurate than that given by the DFT. See the next section for more discussion on the comparison between the FAA and the DFT and FFT.

The FAA was frequently used for evaluating DFT before the invention of FFT (e.g. Bartels, 1935). It was also used for studying periodical phenomena of which the periods are not submultiples of the time series, such as for example, variation of geomagnetic field (Bartels, 1935; Pollak, 1930) and tides (Darwin's method of tidal analysis, see Melchior (1978) for example). As the FFT became so popular soon after its invention, the FAA is no longer much emphasized in modern literatures since then. Recently, a slight variant of it was also used to detect nonharmonic periodicities in biology (the linear stacking method of Hoenen et al. (2001)). In this work we propose to use FAA for precisely determining periods of harmonic signals by intensive search, since periods are required to be determined as precisely as possible in various problems, such as for example, the free oscillation of the Earth. Illustrative example of numerical computation is made for determining some periods of the Earth's free oscillation using a time series of gravity observed by the SG of GeoForschungsZentrum Potsdam (GFZ) installed in Sutherland, South Africa after the 2001 Peruvian Earthquake. A review on the study of the Earth's free oscillation using the worldwide network of SGs in the frame of Global Geodynamics Project (GGP) was given recently by Widmer-Schmidrig (2003).

In fact, the intensive search of periods based on the FAA requires a lot of computation. However, this is not a problem nowadays due to the advance in digital computers.

Another method which is closely related to the FAA is the phasor-walkout method, also known as graphical Fourier transform, summation dial, complex demodulation (Bartels, 1935; Bolt and Brillinger, 1979; Zürn and Rydelek, 1994). This method is particularly suitable for testing if a certain periodicity exists in a time series (Bolt and Brillinger, 1979; Zürn and Rydelek, 1994), though it can be used to search for periods precisely as well. The FAA can be considered as a variant of the phasor-walkout method for searching for periodicities with some approximation in amplitude and phase in favor of quick evaluation. More explanation on their relation will be given in next section.

Based on our analysis and numerical test, we recommend the FAA, which has a fairly simple algorithm, as an alternative method, among other methods being used, for example, the autoregressive method (e.g. Chao and Gilbert, 1980) and its variant, the Sompi method (e.g. Hori et al., 1989), the method of fitting a resonance function to the Fourier spectrum (Bolt and Brillinger, 1979; Dahlen, 1982; Masters and Gilbert, 1983), the interpolated FFT (IFFT) method, the iterative phase average (IWPA) method and the ESPRIT method (e.g. Santamaría et al., 2000) etc, for retrieving periodical signals from time series, and determining their periods with high accuracy. It is expected that it would find additional applications in geophysics.

## 2 The folding-averaging algorithm

For identifying possible sinusoidal signals in a time series, an amplitude spectrum is to be built. The basic principle is to estimate, for every one of an array of preassumed test periods, the amplitude and phase using the FAA. This section is divided into two subsections. The first one explains how to estimate the amplitude and phase of a signal with known period. The second one explains how to build the amplitude spectrum and accurately estimate the periods of the possible signals.

We make two assumptions on the time series: (1) the length of the time series is at least as long as tens or hundreds of the periods of the signals to be studied, (2) the sampling interval is at least as short as a tenth of the periods of the signals to be studied. These assumptions are fulfilled in numerous cases in contemporary geophysical researches.

### 2.1 Estimation of amplitude and phase of a signal with known period

Assume that a signal with known period  $T$  is present in the time series being analyzed and we are estimating the amplitude and phase of the signal.

First of all we analyze an ideal case that the sampling interval  $\Delta t$  can divide the period  $T$  exactly, i.e., the number of observation data in every period,  $(T/\Delta t)$ , is integral. We denote with  $V_0, V_1, V_2, \dots$  the data in the original time series sampled at equally spaced time  $t = 0, \Delta t, 2\Delta t, \dots$ . Denote with  $M$  the number of short time series, each of them having  $N_s = (T/\Delta t)$  data (the length of the test period), that can be cut from the original time series, discarding a small fraction shorter than the test period at the end of the original time series if exists. Arrange the short time series row by row as shown in Table 1. The averaged short time series  $\bar{R}_0, \bar{R}_1, \dots, \bar{R}_{N_s-1}$  is then obtained by averaging every column of the table,

$$\bar{R}_j = \frac{1}{M} \sum_{k=0}^{M-1} V_{k(T/\Delta t)+j}, \quad (1)$$

as the values of the signal in all elements of the same column are the same.

Table 1: Short time series row by row

$V_0$	$V_1$	$\dots$	$V_{N_s-1}$
$V_{(T/\Delta t)}$	$V_{(T/\Delta t)+1}$	$\dots$	$V_{(T/\Delta t)+N_s-1}$
$\vdots$	$\vdots$	$\vdots$	$\vdots$
$V_{(M-1)(T/\Delta t)}$	$V_{(M-1)(T/\Delta t)+1}$	$\dots$	$V_{(M-1)(T/\Delta t)+N_s-1}$

We remark that (1) may be modified to take into account missing data or gaps in the time series by averaging only the data present (excluding the missing data in the sum, and replacing  $M$  by  $M$  minus the number of missing data).

In Table 1, we have not written the subscript of the first data in the short times series,  $k(T/\Delta t)$ ,  $k = 0, 1, \dots, M - 1$ , as  $kN_s$ , because they will be different in the case when  $T/\Delta t$  is not an integral number discussed later.

As the length of the times series is assumed to be much longer than the period of the signal,  $M$  is very large. Thus, in the averaging process, signals with different periods other than  $T$  is practically averaged out. (In fact, signals of which the periods are submultiples of  $T$  remain in the averaged short time series. This problem will be discussed later. Now we simply assume such case does not appear.)

The random error in the averaged short time series is much less than that in the original time series. Denote the root mean square error of the observations in the original time series with  $\sigma$ . The root mean square error of the average values in the short time series is then

$$m = \sigma / \sqrt{M - 1} \quad (2)$$

By assumption,  $M$  is very large. If we have  $M = 100$ , the signal to noise ratio of the averaged short time series is theoretically about 10 times of the original time series. If we have  $M = 10000$ , this value raises to 100.

As signals with different periods are averaged out, and the signal to noise ratio is drastically enhanced, the averaged short time series should be in fact almost a sinusoidal curve, as indicated by numerical examples in the next section.

The amplitude and phase can be estimated using the averaged short time series, of which the signal to noise ratio is assumed to be raised to reasonable level. Express the signal as

$$s(t) = a \sin[(2\pi/T)t + \phi] \quad (3)$$

which is the same form for the original as well as the averaged short time series. The basic relations for determining amplitude and phase are

$$\int_0^T s(t) \begin{Bmatrix} \sin \\ \cos \end{Bmatrix} [(2\pi/T)t] dt = \frac{T}{2} a \begin{Bmatrix} \cos \\ \sin \end{Bmatrix} \phi. \quad (4)$$

As the sampling interval is assumed much shorter than the period of the signal, we can evaluate the integral in the above equation numerically using the left Riemann sum (which is identical to the Trapezoid sums due to the periodicity), replacing the discrete values of  $s$ ,  $s(k\Delta t)$ , with  $\bar{R}_k$ , to obtain estimates for  $a \cos \phi$  and  $a \sin \phi$ :

$$a \begin{Bmatrix} \cos \\ \sin \end{Bmatrix} \phi = \frac{2}{T} \Delta t \sum_{k=0}^{N_s-1} \bar{R}_k \begin{Bmatrix} \sin \\ \cos \end{Bmatrix} [(2\pi/T)(k\Delta t)]. \quad (5)$$

Estimates of amplitude and phase can then be computed according to

$$a = \sqrt{(a \sin \phi)^2 + (a \cos \phi)^2}, \quad \phi = \text{atan2}(a \sin \phi, a \cos \phi) \quad (6)$$

where the function  $\text{atan2}(x, y)$  is provided in practically all programming languages.

In the above formulation, we assumed that the sampling interval  $\Delta t$  divides the period  $T$  exactly, i.e., the number of observation data in every period,  $(T/\Delta t)$ , is integral. But in practice, this rarely happens. As a result, we abandon this assumption. In the more general situation, the expressions  $N_s = T/\Delta t$  and  $k(T/\Delta t)$ ,  $k = 0, \dots, M - 1$ , in the subscripts of data in the short time series listed in Table 1 and equation (1) are no longer integral. Like Darwin's method of tidal analysis (e.g. Melchior, 1978), we replace  $N_s = T/\Delta t$  and  $k(T/\Delta t)$  with the integers closest to them, and still build the averaged short time series according to equation (1). We see that the values of the signal in the elements of the same column in Table 1 are no longer the same, but shifted in phase. Fortunately, the phase shifts between the corresponding elements of any two rows (each row is a short time series) are the same. Hence, in the averaged short time series, this phase shift does not influence the period, but only influences the estimates of amplitude and phase. As we assumed that the sampling interval is much smaller than the period of the signal, the phase shift is small, and thus its influences on the estimates of amplitude and phase are also small. The level of this influence will be formulated in the next subsection.

Finally, we discuss the relation between the FAA and the phasor walkout method. In the phasor walkout method, the expression  $\sum_{k=0}^{N-1} V_k \exp\{-i(2\pi/T)k\Delta t\}$  is evaluated graphically for any test period  $T$ , where  $N$  is the total

number of data in the original time series, and  $i = \sqrt{-1}$  (e.g. Zörn and Rydelek, 1994). It can be readily seen that the same expression is evaluated in the FAA outlined above (apart from a common multiplier and the approximation due to the small phase shifts in the FAA), but expressed in terms of amplitude and phase (e.g. Bartels, 1935).

## 2.2 Amplitude spectrum and accurate determination of periods

Now we assume that sinusoidal signals exist in a time series, but the periods are not known, and the study is intended to identify the periods.

We begin by analyzing the signature of a sinusoidal signal, of which the exact value of period  $T_E$  is not known, in the averaged short time series built with a test period  $T$ . We denote with  $\Delta T$  the difference between  $T$  and  $T_E$ , so that

$$T = T_E + \Delta T. \quad (7)$$

The formula of the signal is the same as (3), but with  $T$  replaced by  $T_E$ . For clarity, we rewrite it out:

$$s(t) = a \sin[(2\pi/T_E)t + \phi]. \quad (8)$$

Evidently, the signature of this signal in the averaged value  $\bar{R}_j$  given by equation (1) is

$$\bar{s}_j = \frac{1}{M} \sum_{k=0}^{M-1} a \sin\{(2\pi/T_E)[k(T/\Delta T) + j]\Delta T + \phi\} \quad (9)$$

which can be further written as

$$\bar{s}_j = \frac{1}{M} \sum_{k=0}^{M-1} a \sin[(2\pi/T_E)(j\Delta T + k\Delta T) + \phi]. \quad (10)$$

We see that  $\bar{s}_j$  is the average of the values of the sinusoidal signal at  $M$  nodes equally spaced by  $\Delta T$ :  $j\Delta T, j\Delta T + \Delta T, \dots, j\Delta T + (M-1)\Delta T$ . When  $\Delta T$  is very small as compared to  $T_E$ , it can also be understood as the average value of the signal in the interval between the epochs  $j\Delta T$  and  $j\Delta T + M\Delta T$ . There are two possibilities for the result of (10).

1. According to (10), the values of the signal at all of the  $M$  nodes are equal to its value at  $t = j\Delta T$  when  $\Delta T = 0, T_E, 2T_E, \dots$ . Hence, the value of  $\bar{s}_j$  is also equal to the value of the signal at  $t = j\Delta T$ . So, if a signal with a period  $T_E$  is present in the time series, and if we have built the average short time series for test periods  $T = T_E, 2T_E, \dots$ , all the averaged short time series contains the signal. Reversely, this means that, in the averaged short time series built with a test period  $T$ , there may be a signals with periods  $T, T/2, T/3, \dots$ . But when we use (5) and (6) to estimate amplitude and phase, the results obtained are just of those of the signal with period  $T$ , the signals with periods  $T/2, T/3, \dots$  have no contribution to the results, a direct consequence of the orthogonality of the trigonometric functions.
2. Otherwise,  $\bar{s}_j \rightarrow 0$  when  $M \rightarrow \infty$ . This result is a consequence of the fact that the average of a sinusoidal signal in any time interval equal to its period is equal to zero. In practice,  $M$  is always a finite number. and hence  $\bar{s}_j$  can not really vanish. According to what was stated below (10), we see that  $\bar{s}_j$  does vanish when  $M\Delta T = T_E, 2T_E, \dots$ . So in the spectrum built, small sidelobes appear around the highest central peak representing the signal, the larger is  $M$ , the smaller the sidelobes.

Based on the above properties, we can design a process for searching for periods of possible signals: estimating the amplitude  $a$  according to (5) and (6) for an array of test period  $T$ :  $T_0, T_1 = T_0 + dT_0, T_2 = T_1 + dT_1, \dots$ , the periods of possible signals are the one which have maximum extreme values of  $a$ . But we have to answer another question: what are the favorite values of  $dT_0, dT_1, \dots$  in the computation? If the values of  $dT_0, dT_1, \dots$  are too large, we may not see the maximum extreme of the estimate of  $a$  at all. The choice of  $dT_0, dT_1, \dots$  depends on the accuracy we expect. Take reference to (10) again. If  $T_E$  is in a interval  $[T_k, T_{k+1}]$ , for the estimate of  $a$  at  $T_k$  or  $T_{k+1}$  to be significantly distinguishable as nearly maximum extreme,  $\Delta T = T_{k+1} - T_E$  or  $\Delta T = T_k - T_E$  must be small enough in magnitude. We see that the absolute values of either  $\Delta T = T_{k+1} - T_E$  or  $\Delta T = T_k - T_E$  should be smaller than  $dT_k/2$ . So, in the search of signals, we choose  $MdT_k/2 \geq M\Delta T$  to be only a small portion of  $T_k$  (or  $T_{k+1}$ ). The smaller this value is, the clearer the maximum extreme we see. We chose  $MdT_k/2$  to be only one  $n$ -th of  $T_k$ , whence

$$dT_k = 2T_k/(nM). \quad (11)$$

This implies that  $\bar{s}_j$  given in (10) is the average of the value of the signal at  $M$  equally spaced nodes in a interval of which the length is at maximum one  $n$ -th of the test period (see the analysis below equation (10)). The practical computation for the search of signals and accurate determination of periods is done in two steps:

1. Build a less accurate amplitude spectrum by choosing  $n$  to be moderately large, for example, between 4 to 16. Peaks in the spectrum may represent signals;
2. Pick out the peaks and search intensively for the maximum extremes of the amplitude near the peaks by setting  $n$  to its maximum meaningful value to be discussed below.

For any signal with a period  $T_E$ , we can not expect that  $T_E/\Delta t$  be integral. Thus the approximation by phase shifting as mentioned in the last subsection should always be assumed. So, making the interval  $M\Delta T \leq MdT_k/2$  smaller than the the possible unavoidable phase shift is meaningless. The phase shifts may be as large as  $\Delta t/2$  to both the left and right sides. So the smallest meaningful value for  $MdT_k/2$  is  $\Delta t$ . This implies that the maximum theoretical resolution for period is  $dT_k = 2\Delta t/M$ , which is approximately  $2(T_k/L_{TS})\Delta t$  as mentioned in the introduction, as  $M$  is approximately  $L_{TS}/T_k$ . The value for  $n$  is then  $T_k/\Delta t$ . This ideal resolution may be achieved only under the ideal situation that only one signal is present in the times series and there is no error of observation. This is certainly not the case in practice. Unfortunately, we can not give an adequate estimate of error in the periods found using this method, just the same as the phasor walkout method (Zürn and Rydelek, 1994). The issue of precision will be discussed later. The interval of period in which signals are sought is chosen based on our a-priori knowledge on the problem studied.

The estimates of phase and amplitude using the FAA are not those of the original time series, but of the averaged short time series. In this paragraph we study the differences between the phase and amplitude of the original time series and the averaged short time series. These differences represent the minimum errors of the estimates using the FAA. We know from the statement after (10) that the value of the averaged short time series at epoch  $j\Delta t$ ,  $\bar{s}_j$ , can be understood as the average of the real signal between the epochs  $j\Delta t$  and  $j\Delta t + M\Delta T$ , where  $\Delta T$  is the difference between the test period  $T$  and the real period of the signal  $T_E$  defined in (7). Now we assume that  $\bar{s}_j$  is the value of a sinusoidal curve  $\bar{s}(t)$  at the epoch  $t = j\Delta t$ . According to the FAA,  $\bar{s}(t)$  is the approximation of the signal  $s(t)$ , and  $\bar{s}(t)$  can be understood as the average of  $s(t)$  in the interval between the epochs  $t$  and  $t + M\Delta T$ . According to this relation, we can analyze the signature of the phase and amplitude of  $s(t)$  in  $\bar{s}(t)$ . We assume  $s(t)$  attains its maximum extreme  $a$  at  $t = t_m$ , i.e.  $(2\pi/T_E)t_m + \phi = \pi/2$ . It can then be seen that  $\bar{s}(t)$  attains its maximum extreme at the epoch  $t = t_m - M\Delta T/2$ , since at this epoch  $\bar{s}(t)$  is the average of  $s(t)$  in the interval between the epochs  $t_m - M\Delta T/2$  and  $t_m + M\Delta T/2$  containing  $t_m$  as midpoint. So the phase of  $\bar{s}(t)$ ,  $\bar{\phi}$ , is  $(2\pi/T_E)(M\Delta T/2) = \pi M\Delta T/T_E$  in advance (as the maximum arrives earlier) compared to that of  $s(t)$ , i.e.

$$\bar{\phi} = \phi + \pi M\Delta T/T_E. \quad (12)$$

The amplitude of  $\bar{s}(t)$ ,  $\bar{a}$ , is the maximum extreme of  $\bar{s}(t)$  which can be obtained to be

$$\bar{a} = [(aT_E)/(\pi M\Delta T)] \sin[(2\pi/T_E)(M\Delta T/2)]. \quad (13)$$

These relations of phase and amplitude can be used to estimate errors of phase and amplitude of the signals obtained using the FAA.

Now we turn to analyze the errors of amplitude and phase of a real signal in the FAA spectrum. Imagine that  $T_E$  falls in between the test periods  $T_k$  and  $T_{k+1}$ . The estimate of period is then  $T_k$  or  $T_{k+1}$  depending on to which one  $T_E$  is closer, and  $\Delta T = T_k - T_E$  at  $T_k$ ,  $\Delta T = T_{k+1} - T_E$  at  $T_{k+1}$ . The phase and amplitude of  $\bar{s}(t)$  are, according to (12) and (13),

$$\bar{\phi}_k = \phi + \pi M(T_k - T_E)/T_E, \quad (14)$$

$$\bar{a}_k = \frac{aT_E}{\pi M(T_k - T_E)} \sin \left\{ \left( \frac{2\pi}{T_E} \right) \left[ \frac{M(T_k - T_E)}{2} \right] \right\} \quad (15)$$

at  $T_k$ , and

$$\bar{\phi}_{k+1} = \phi + \pi M(T_{k+1} - T_E)/T_E, \quad (16)$$

$$\bar{a}_{k+1} = \frac{aT_E}{\pi M(T_{k+1} - T_E)} \sin \left\{ \left( \frac{2\pi}{T_E} \right) \left[ \frac{M(T_{k+1} - T_E)}{2} \right] \right\} \quad (17)$$

at  $T_{k+1}$ . Noticing  $T_k \leq T_E \leq T_{k+1}$ , we see that the estimate of phase is in backward at  $T_k$ , and in advance at  $T_{k+1}$  as compared to that of the signal  $s(t)$ . Consider the worst situation that  $T_E$  is at the midpoint between  $T_k$  and  $T_{k+1}$ , i.e.  $T_k - T_E = -dT_k/2$ ,  $T_{k+1} - T_E = dT_k/2$ . Then, by using (11), we see that the phase and amplitude are

$$\bar{\phi}_k = \phi - (2\pi/T_E)[T_k/(2n)], \quad (18)$$

$$\bar{a}_k = \{(aT_E)/[\pi T_k/n]\} \sin\{(2\pi/T_E)[T_k/(2n)]\} \quad (19)$$

at  $T_k$ , and

$$\bar{\phi}_{k+1} = \phi + (2\pi/T_E)[T_k/(2n)], \quad (20)$$

$$\bar{a}_{k+1} = \{(aT_E)/[\pi T_k/n]\} \sin\{(2\pi/T_E)[T_k/(2n)]\} \quad (21)$$

at  $T_{k+1}$ . In (18) to (21), setting  $T_k = T_E$  gives good approximations. So we have

$$\bar{\phi}_k = \phi - \pi/n, \quad (22)$$

$$\bar{a}_k = (na/\pi) \sin(\pi/n) \quad (23)$$

at  $T_k$ , and

$$\bar{\phi}_{k+1} = \phi + \pi/n, \quad (24)$$

$$\bar{a}_{k+1} = (na/\pi) \sin(\pi/n) \quad (25)$$

at  $T_{k+1}$ . These relations give the differences between  $a$  and  $\bar{a}$ , and  $\phi$  and  $\bar{\phi}$ , which represent the highest precision in the estimates using FAA for any chosen value of  $n$ . This precision may be attained only at the extremely ideal situation: only one signal is present in the time series, and the observation is error free, just like the situation for attaining the maximum precision for period. One can easily estimate the precision when highest resolution in period is made by setting  $n = T_k/\Delta t$ .

In practice, the time series may be more complicated. For example, it may contain linear tendency which perturbs the estimate of  $a$  and makes it unclear as maximum extreme at the period  $T_E$ . In the averaged short time series, residuals form signals of longer periods not cancelled by averaging are also similar to linear tendency, or even like a quadratic curve. So, it is preferable that signals outside the interval of interest be filtered out before using the FAA.

For having more accurate estimates of  $a$  and  $\phi$ , or for having error estimates for them, instead of using (5) and (6), a least square fit of the averaged short time series by a sinusoidal curve with the period found may be used. This may be done either by using the cosiner algorithm (Nelson et al., 1979) or by linearizing the problem using the estimates of  $a$  and  $\phi$  according to (5) and (6) as initial guess. A linear, and even a quadratic curve, may be combined with the sinusoidal curve for reducing the errors of estimates. Nevertheless, the error estimates represent the misfit to the averaged short time series, but not the original time series, as already discussed.

The same as the phasor walkout method (Zürn and Rydelek, 1994), we can not give adequate estimates of errors in the periods found using this method, which is already mentioned earlier in the text. In this work we propose to use an indirect method to infer errors in the estimates of periods. First, we do the analysis for the time series. Second, according to the periods, amplitudes and phase of the signals found, we add into the time series some synthetic signals which are similar to the signals found in the first step, but with periods slightly shifted for not overlapping with the signals. And third, redo the analysis for the time series containing the synthetic signals. For the synthetic signals, as the exact values of their periods, amplitudes and phases are known, the absolute errors of their estimates may be determined. These absolute errors of the estimates of the synthetic signals can then serve as a good reference of errors for the estimates of the real signals.

### 2.3 Relation with the DFT and the FFT with zero padding

First we discuss the relation between the FAA and the DFT. In the DFT, the coefficients of the complex fourier series of the time series are  $(1/N) \sum_{j=0}^{N-1} V_j \exp\{-i(2\pi/T_k)j\Delta t\}$ , where  $N$  is the total number of data in the time series,  $i = \sqrt{-1}$  and  $T_k = L_{TS}/k$ . This is the same as the FAA if  $T_k = L_{TS}/k$  is chosen as the test period (notice that we used the amplitudes and phases of the sine functions in the FAA). So, if we chose  $\dots, L_{TS}/3, L_{TS}/2, L_{TS}$ , i.e. the periods of the sinusoidal functions used in DFT, as test periods for the FAA, the FAA spectrum is identical to the DFT spectrum (apart from the approximation due to the small phase shifts in the FAA). So their difference lies on the differences of nodes of periods of the spectrums built using the two methods respectively. The nodes of periods of the FAA spectrum was given by (11) which may be made as dense as one want by choosing the value of  $n$  large enough, without exceeding the limit of maximum resolution as discussed before. For the DFT spectrum, the nodes of periods are submultiples of the length of the time series. Hence, at any node  $T = L_{TS}/k$ , the step to the next node is

$$dT = L_{TS}/(k-1) - L_{TS}/k = T/(k-1). \quad (26)$$

Notice that the meaning of  $k$  is similar to that of  $M$  in (11), i.e. the number of periods in the times series. So, when  $k$  or  $M$  is large, and when  $n$  in (11) is set to 2 for the FAA, the distances between two nodes for the DFT spectrum is the same order of magnitude as that of the FAA spectrum at comparable nodal periods in the two spectra. However, Even when  $n$  in (11) is set to 2 for the FAA, the nodal periods of the DFT and FAA spectrums are not necessarily equal because the choice of test periods for the FAA is not unique like DFT. Thus we conclude that, when the value of  $n$  in (11) is set to 2, the FAA gives a spectrum with practically the same resolution of period as the DFT. The precision of phase and amplitude of the FAA discussed above also applies to DFT by setting  $n = 2$ . So, according to (22) to (25), we can also conclude that, the largest possible errors in the estimates of phase and amplitude in DFT may attain  $\pi/2$

and  $[(\pi - 2)/\pi]a = 0.36a$  even if the observation is error free. This represent in fact the DFT precision in phase and amplitude, while  $dT/2 = T/[2(k - 1)]$  represents the DFT precision in period.

Since its invention, the FFT has being used extensively to evaluate the DFT. Here, for illustrative purpose, we assume without loosing generality that the FFT requires the total number of data in a time series to be power of 2 (though this is not a prerequisite of the FFT). If the criteria is not satisfied, zeros are customarily added by the end of the time series to the length required, called zero padding. Now we continue to use  $N$  to denote the total number of data in the original times series, and to use  $N'$  to denote the total number of data (that is power of 2) after zero padding, i.e.  $N' - N$  zeros are added to end of the original time series. In the FFT, the coefficients of the complex fourier series of the zero-padded time series are  $(1/N') \sum_{j=0}^{N'-1} V_j \exp\{-i(2\pi/T_k)j\Delta t\}$ , where  $T_k = L'_{TS}/k$ ,  $L'_{TS}$  being the length of the zero-padded time series. Remembering that  $V_j$  is equal to zero when  $N \leq j < N'$ , we can readily see that, if we chose  $\dots, L'_{TS}/3, L'_{TS}/2, L'_{TS}$ , i.e. the periods of the sine functions used in the FFT, as test periods for the FAA, the FAA spectrum is identical to the FFT spectrum multiplied with the factor  $N'/N$  (apart from the approximation due to the small phase shifts in the FAA). So, the same as the FAA, the FFT can also be used to build spectrums with high resolution of period of signals by padding the time series with a lot of zeros (Santamaría et al., 2000). But the FAA is superior for accurate determination of the periods of the signals by extensive search near the peaks of the spectrums built (the second step of accurate determination of periods stated in the last subsection), since achieving the highest resolution that the FAA can attain using the FFT requires a huge amount of computation (though possible).

Due to the above relation of the FAA to the DFT and FFT, we can apply tapers to the FAA in the same way as to the DFT and FFT.

### 3 Application for the determination of the periods of the Earth's free oscillation using SG data

In this section we apply the FAA to estimate some periods of the Earth's free oscillation using SG data. The objective is to demonstrate the applicability of the FAA. The detail of the subject itself on the study of the Earth's free oscillations using the worldwide network of SGs in the frame of GGP is referred to the recent review by Widmer-Schmidrig (2003).

A property of the Earth's free oscillations, the decay, was not considered in the last section in building the FAA. A decaying sinusoidal signal can be written as (Zürn and Rydelek, 1994)

$$s(t) = a \exp\{-[\pi/(QT)]t\} \sin[(2\pi/T)t + \phi] \quad (27)$$

where  $Q$  is the quality factor. It is straightforward to redo the formulation in the last section while replacing (3) with this signal. The main characteristics of the conclusion may be inferred by inspection. As the decaying factors of the signal of period  $T$  in all the short time series in Table 1 are the same, they can be safely averaged, obtaining as result an averaged short time series which contains mainly this signal. But the amplitude of the signal in the averaged short time series is the average all over the original time series. We have also attempted to recover the quality factor by fitting the averaged short time series with the decaying signal. This seems impossible because the difference in amplitude in one cycle is too small as the quality factor  $Q$  is large in general. There are spectral analysis methods specifically conceived for retrieving decaying signals like the Earth's free oscillation (e.g. Bolt and Brillinger, 1979; Chao and Gilbert, 1980; Dahlen, 1982; Masters and Gilbert, 1983; Lindberg and Park, 1987; Park et al., 1987; Hori et al., 1989). The FAA is understood as an independent method for period determination. For determining periods of decaying signals, we cannot use too long time series, since, when the amplitude of the signal become too small, using more data implies adding more noise. Dahlen (1982) recommended that the length of the time series be  $Q$  cycles of the signal to be recovered.

The main Peru Earthquake of magnitude 8.4 occurred on 20:33:14 UTC, 23 June, 2001. Aftershocks of magnitudes 6.7, 6.6 and 7.6 occurred on 04:18:31 UTC, 26 June, 13:53:48 UTC, 5 July and 09:38:43 UTC, 7 July, respectively. The gravity time series is sampled at 5 seconds interval, which is first filtered using the least squares band pass filter of TSoft provided by the Royal Observatory of Belgium (<http://www.observatoire.be/SEISMO/TSOFT/tsoft.html>), to retain signals only between 0.15 to 2 mHz. Then the air pressure effect is corrected using a frequency dependent method (e.g. Neumeyer, 1995), as this effect may be important for the low frequency or long period free oscillation band (Van Camp, 1999; Zürn and Widmer, 1995). Therefore the 5 sec air pressure data is filtered the same way, and a transfer function between the air pressure and gravity data is calculated using blocks of length 12 hours. This transfer function is multiplied to the Fourier spectrum of the air pressure data which is then subtracted from the gravity data Fourier spectrum. The corrected gravity data are finally received using the inverse Fourier transformation. We do see significant improvement of signal to noise ratio under 1.3 mHz. The time series finally used in this study after filtering and air pressure correction is from 08:00:00 UTC on June 24 to 02:00:00 UTC on July 4, its length being 234 hours. Based on a visual inspection of the spectra built using the data of various time spans, the noise level has the lowest noise level.

Table 2: Synthetic signals added into the time series. They will serve as a tool to estimate the precision of the estimates of periods by comparing the assigned and estimated values of them.

Mode	Period s	Initial amplitude $\text{nm s}^{-2}$	Quality factor	Initial phase
${}_0W_0$	1303.000	0.0047	5700	1.0
${}_1W_0$	596.000	0.0026	1800	2.0
${}_0W_2^{-2}$	2942.000	0.0024	500	2.0
${}_0W_2^{-1}$	2902.000	0.0013	500	1.0
${}_0W_2^0$	2864.000	0.0002	500	0.0
${}_0W_2^1$	2826.000	0.0030	500	-1.0
${}_0W_2^2$	2792.000	0.0018	500	-2.0

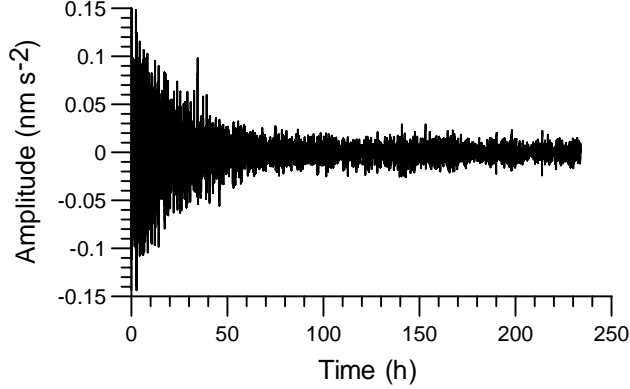


Figure 1: The Sutherland SG gravity time series after the 2001 Peruvian earthquake after bandpass filtering and atmospheric pressure correction used in the study. The initial time corresponds to 08:00:00 UTC on June 24, and the end time corresponds to 02:00:00 UTC on July 4. The length is 234 hours. Based on a visual inspection of the spectra built using the data of various time spans, the noise level has the lowest noise level. The synthetic signals listed in Table 2 have been added to the gravity time series.

We use  ${}_0S_0$ ,  ${}_1S_0$  and  ${}_0S_2$  to test the method. The modes  ${}_0S_0$  and  ${}_1S_0$  are the simplest because each of them has only one singlet in the spectrum. The mode  ${}_0S_2$  is split into five singlets  ${}_0S_2^m$ ,  $m \in \{-2, -1, 0, 1, 2\}$ .

As proposed in the last section, the precision of estimates of periods will be inferred by comparing the exact and estimated values of periods of similar synthetic signals added into the time series. The synthetic signal corresponding to a real signal is chosen as similar as possible to the real signal in property, except for a small difference in periods, necessary for distinguishing them in the spectrum. For conformance with the damping nature of free oscillation, the quality factor  $Q$  is also considered in each of these synthetic signals, though we don't estimate  $Q$  using FAA. The synthetic signals corresponding to  ${}_0S_0$ ,  ${}_1S_0$  and  ${}_0S_2$  are  ${}_0W_0$ ,  ${}_1W_0$  and  ${}_0W_2$ , where  ${}_0W_2$  is also split into five singlets like  ${}_0S_2$ ,  ${}_0W_2^m$ ,  $m \in \{-2, -1, 0, 1, 2\}$ . We chose the periods and quality factors of  ${}_0W_0$  and  ${}_1W_0$  respectively to be close to those of  ${}_0S_0$  and  ${}_1S_0$  given by Riedesel et al. (1980). The choice of  ${}_0W_2^m$ ,  $m \in \{-2, -1, 0, 1, 2\}$  is more sophisticated, as the property of splitting of  ${}_0S_2$  should be retained. We chose their periods by shifting the frequencies of  ${}_0S_2^m$ ,  $m \in \{-2, -1, 0, 1, 2\}$  given by Rosat et al. (2003a) by about the same amount, and their quality factors to be close to that of  ${}_0S_2$  given by Dziewonski and Anderson (1981). For all the synthetic signals, the initial amplitudes are chosen to be close to those of the corresponding real signals determined by analyzing the time series without the synthetic signals, and the phases, arbitrarily. The parameters chosen for the synthetic signals are listed in Table 2. The graph of the time series with synthetic signals added is shown in Figure 1.

As mentioned in the last section, we search for periods in two steps. Firstly, we build an amplitude spectrum between 0.2 and 2 mHz by setting  $n = 16$ . Secondly, we pick out the peaks from the spectrum and search more accurately for the periods around these peaks by setting  $n = T_k/\Delta t$ , representing maximum possible resolution. Here we add a third step: estimate the amplitudes and phases using least squares fits to the averaged short time series built using the periods determined in the second step. The amplitude spectrum built at first step is shown in Figure 2. The splitting of  ${}_0S_2$  and  ${}_0W_2$  is shown in Figure 3, which is the amplification of a portion of Figure 2. As illustration, we also present the graphs of the averaged short time series of  ${}_0S_0$  and  ${}_1S_0$  in Figure 4, which are indeed quite similar to sinusoidal curves. The results from the second and third steps are listed in Table 3. As the quality factor is not estimated in our approach, the amplitudes we obtain represent only the average, thus not comparable with the initial values as given in Table 2. Nevertheless, we still listed them in the table. More digits are given for comparison between

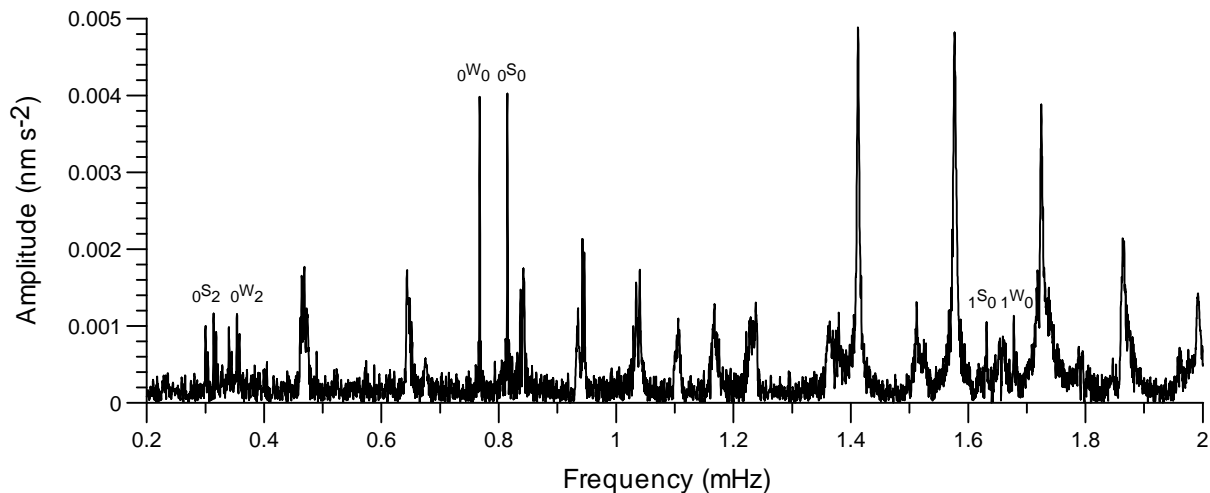


Figure 2: The amplitude spectrum of the gravity time series shown in Figure 1 built using the FAA. The peaks  ${}_0S_0$ ,  ${}_1S_0$  and  ${}_0S_2$  are the free oscillation modes studied as examples in this work. The peaks  ${}_0W_0$ ,  ${}_1W_0$  and  ${}_0W_2$  are the corresponding synthetic signals added to the time series for assessing precision of the estimates of periods by comparing the assigned and estimated values of them.

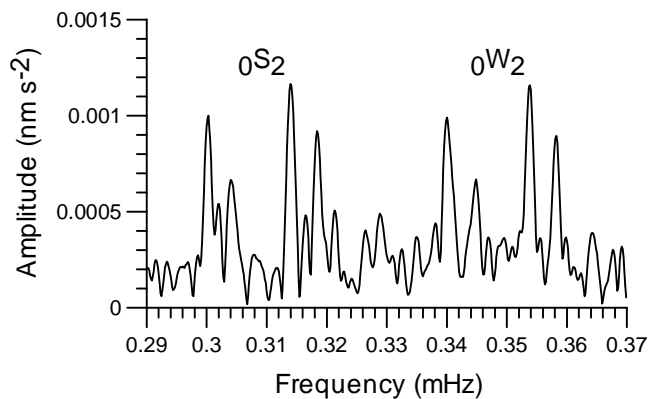


Figure 3: The splitting of  ${}_0S_2$  (left) and  ${}_0W_2$  (right). This is a portion of the Figure 2 enlarged for showing the detail in this band.

the estimates of the parameters and errors. The results in the table will be discussed in more detail in the following two paragraphs.

First, we discuss the results for  ${}_0S_0$  and  ${}_1S_0$ . Levels of error in the estimates of their periods are inferred from comparing the assigned and estimated periods of the synthetic signals  ${}_0W_0$  and  ${}_1W_0$  listed in Tables 2 and 3, which are lower than 50 ppm for both of them. As the maximum resolution of periods of the FAA as discussed in the last section is far more accurate, this level of error is the result of the overall influence of all other signals and random errors in the time series. For the Earth's free oscillation, the estimates of the period of a mode obtained using different data should be the same. Here we compare our results with those of Riedesel et al. (1980) who stacked 9 IDA records, and estimated the period of  ${}_0S_0$  to be  $1227.500 \pm 0.005$  (or  $\pm 4$  ppm) seconds using a time series of 2000 hours, and the period of  ${}_1S_0$  to be  $612.929 \pm 0.018$  (or  $\pm 30$  ppm) seconds using a time series of 300 hours. We see that our results are in close agreement with those of Riedesel et al. (1980).

In this paragraph, we discuss the results of the 5 singlets of the mode  ${}_0S_2$ . For both  ${}_0S_2$  and  ${}_0W_2$ , the singlets corresponding to the values of the azimuthal order number  $m = -2, -1, 0, 1, 2$  are from left to right in Figure 2. We see that the  $m = 0$  singlets of them cannot be clearly seen. Rosat et al. (2003a) gave in their Figure 5 the same graph for  ${}_0S_2$  obtained using the data of the Strasbourg SG after the same Earthquake, where the singlet of  $m = 0$  can be clearly seen. But when we compare the spectrums from the Sutherland and Strasbourg SG data in their Figure 4, we see that the singlet of  $m = 0$  for the Sutherland instrument can neither be clearly seen. In fact, the amplitude of the singlets of  ${}_0S_2$  with azimuthal number  $m = -2, -1, 0, 1, 2$  depend on the amplitude of  $P_2^m(\cos \theta)$  ( $\theta$  is the colatitude) that is respectively 0.18, 0.23,  $-0.07$ ,  $-1.36$ , 2.14 at Sutherland, and 0.11,  $-0.25$ , 0.34, 1.49, 1.31 at Strasbourg. We see that the magnitude of  $P_2^0(\cos \theta)$  at Sutherland is only one fifth of that at Strasbourg. So we attribute this low

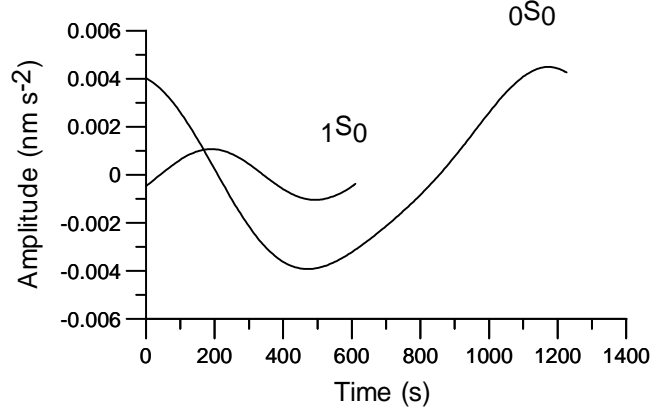


Figure 4: The averaged short time series of  ${}_0S_0$  and  ${}_1S_0$  corresponding to the maximum amplitude extremes. They are used for estimating amplitudes and phases. As the modes studied decay, only their average amplitudes can be estimated.

Table 3: Estimates of parameters of the synthetic and real signals. The differences between the amplitudes and phases of the synthetic signals  ${}_0W_0$ ,  ${}_1W_0$  and  ${}_0W_2$  in this table and their corresponding exact values listed in Table 2 serve as error estimates for the free oscillation modes  ${}_0S_0$ ,  ${}_1S_0$  and  ${}_0S_2$ . The amplitudes are not comparable because those listed in Table 2 are the initial values, and those in this table is the average ones. The singlets  ${}_0W_2^0$  and  ${}_0S_2^0$  are too small in amplitudes, and are not estimated.

Mode	Period s	Amplitude nm s <sup>-2</sup>	RMS error nm s <sup>-2</sup>	Phase	RMS error
${}_0W_0$	1303.063	0.003996	0.000027	1.0788	0.0068
${}_1W_0$	596.018	0.001144	0.000003	2.0012	0.0027
${}_0S_0$	1227.509	0.004042	0.000025	2.0167	0.0063
${}_1S_0$	613.010	0.001055	0.000003	-0.3793	0.0029
${}_0W_2^{-2}$	2941.289	0.000984	0.000042	1.9352	0.0429
${}_0W_2^{-1}$	2899.545	0.000632	0.000173	0.6680	0.2744
${}_0W_2^0$	-	-	-	-	-
${}_0W_2^1$	2826.855	0.001134	0.000099	-0.7947	0.0873
${}_0W_2^2$	2791.475	0.000904	0.000026	-2.1804	0.0285
${}_0S_2^{-2}$	3330.855	0.001020	0.000018	-1.7162	0.0181
${}_0S_2^{-1}$	3289.067	0.000638	0.000026	2.0646	0.0404
${}_0S_2^0$	-	-	-	-	-
${}_0S_2^1$	3184.754	0.001121	0.000056	0.4112	0.0499
${}_0S_2^2$	3140.636	0.000922	0.000025	-2.5517	0.0272

Table 4: Comparison between the estimates of the periods of the  ${}_0S_2$  singlets of Rosat et al. (2003b) obtained by fitting a resonance function to each Fourier spectral peak and those obtained using the FAA using the Strasbourg SG data (Unit: second). The first and second lines are respectively the estimates and their errors of Rosat et al. (2003b). The third line is our estimates. And the last line is the disagreement between the estimates of Rosat et al. (2003b) and the ours.

	${}_0S_2^{-2}$	${}_0S_2^{-1}$	${}_0S_2^0$	${}_0S_2^1$	${}_0S_2^2$
Rosat et al.	3334.91	3284.05	3235.72	3186.09	3143.57
	$\pm 0.59$ (177 ppm)	$\pm 0.73$ (222 ppm)	$\pm 0.60$ (188 ppm)	$\pm 0.52$ (163 ppm)	$\pm 0.63$ (200 ppm)
Our results	3336.61	3284.65	3235.19	3185.28	3144.70
Disagreement	$\pm 1.70$ (509ppm)	$\pm 0.60$ (182ppm)	$\pm 0.53$ (164ppm)	$\pm 0.81$ (254ppm)	$\pm 1.13$ (360ppm)

amplitude of the  $m = 0$  singlet of  ${}_0S_2$  to the data of the Sutherland instrument, and is not studied. As  ${}_0W_2$  was made as closer to  ${}_0S_2$  as possible, it is natural that its  $m = 0$  singlet is neither clear in the spectrum. Level of errors in the estimates of the periods of the  ${}_0S_2$  singlets are estimated by comparing the assigned and estimated periods of the  ${}_0W_2$  singlets listed in Tables 2 and 3. We see that the result of  ${}_0W_2^{-1}$  has the largest error, which is 845 ppm. This is conceivable as this singlet has the smallest amplitude. The error level of other singlets are below 300 ppm. For comparison, we list in Table 4 the estimates of for the periods of the  ${}_0S_2$  singlets obtained by Rosat et al. (2003b) using the Strasbourg SG data. Their disagreement from our estimate using the Sutherland SG data listed in Table 3 are 4.06 (1216ppm), 5.02 (1525ppm), 1.34 (419ppm), 2.93 (934ppm) for  $m = -2, -1, 1, 2$  respectively. We see that these differences are large that seems difficult to accept. If we compare the  ${}_0S_2$  spectrum of the Strasbourg SG data given in Figure 2 of Rosat et al. (2003b) with our Figure 2, we see that the Strasbourg spectrum is very clean, but the Sutherland spectrum is polluted by some lower peaks which may be local background noises, or hums. Perhaps, the periods of the Sutherland spectrum are biased by these hums with extremely close periods. For example, for the lowest peak,  ${}_0S_2^{-1}$ , which may be more affected by the hums, our result agrees with that of Rosat et al. (2003a) at 1525 ppm, but for the highest peak,  ${}_0S_2^1$ , which may be less affected by the hums, the agreement is as good as 419 ppm, quite close to our error estimate using synthetic signal.

As supplement of comparison, we have also applied in the same way the FAA to a 228 h-long record of the Strasbourg SG (from 12 O'clock of Jun 25, 2001 to 0 O'clock of July 5, 2001, this time span is chosen such that the noise is lowest in the  ${}_0S_2$  band in the spectrum according to the visual examination). The results are also listed in Table 4. The last row of the table is the disagreements between our results and those of Rosat et al. (2003b), which should be acceptable as compared to the error estimates of Rosat et al. (2003b) since the data sets used are in fact not exactly the same.

As demonstration of the use of taper, we have applied a Hanning window to the same data set used by Rosat et al. (2003b) after least square band pass filtering to keep signals in the range 0.2-0.4 mHz (the band of the mode  ${}_0S_2$ ), and then determined the periods using the FAA. The periods for the 5 singlets of the mode  ${}_0S_2$  for  $m = -2, -1, 0, 1, 2$  are respectively 3334.99, 3283.17, 3235.65, 3186.03, 3142.86 seconds, which are in general closer to the results of Rosat et al. (2003b) than those obtained in the last paragraph (listed in Table 1).

## 4 Concluding remarks

In this work, the FAA is applied to seek periodical signals in time series and to determine their periods accurately. Various aspects of the FAA are discussed, including the signal-to-noise ratio improvement in the averaged short time series, the highest possible accuracy of the estimates of the periods (for an ideal case), the signature of the real signal in the short time series, the errors in the estimates of amplitudes and phases caused by errors in the estimates of periods. The relations of the FAA with the DFT and the FFT with with zero padding are also investigated, showing that tapers can be used for the FAA in the same way as for the DFT and FFT.

A weakness of the FAA is that it does not provide with estimates of errors for the estimates of periods. However, we used an indirect method for assessing the errors of the periods which consists of adding into the time series synthetic signals that are quite similar to the real signals found, and then using the differences between the exact and estimated values of periods of these synthetic signals as a measure of errors for the estimates of periods for real signals.

To test the technique, we have applied it to numerous synthetic time series that consist of sinusoidal signals and random noises of different level. The results demonstrate the feasibility of the method.

For geophysical application, we used it to determine the periods of the Earth's free oscillations using a time series of gravity observed by the GFZ SG installed in Sutherland, South Africa after the 2001 Peru Earthquake. Comparison of our results with previous works are made using the modes  ${}_0S_0$ ,  ${}_1S_0$  and  ${}_0S_2$ . For all the synthetic signals corresponding the these modes added for accessing precision, our estimates of periods show very close agreements with the exact values assigned. Our estimates of periods for  ${}_0S_0$  and  ${}_1S_0$  are also in very good agreements with the very elaborated estimates of Riedesel et al. (1980). But for the mode  ${}_0S_2$ , the the agreement between our estimates of period and the recent estimates of Rosat et al. (2003b) we have chosen for comparison is less good, which may be due to the high noises very close to the frequency of  ${}_0S_2$  in the Sutherland data. We have also applied the FAA to the Strasbourg SG data that Rosat et al. (2003b) used, and the results show very good agreement.

Based on our experiments, we conclude that the FAA as a valuable method, among other methods being used, for retrieving periodical signals from time series and determining their periods with high accuracy. It is expected to find other applications in geophysics.

**Acknowledgment** We gratefully acknowledge B. Ducarme, M. Van Camp and S. Rosat for helpful discussions. S. Rosat has also provided the preprocessed Strasbourg SG data. J.Y. Guo is supported by the Natural Science Foundation of China under grant 40274028.

## References

- Bartels, J., 1935. Random fluctuations, persistence and quasipersistence geophysical and cosmical periodicities. *Terr. Magn. Atmos. Electricity*, 40, 1-60.
- Bolt, B. A., and Brinlinger, D. R., 1979. Estimation of uncertainties in eigenspectral estimates from decaying geophysical time series. *Geophys. J. R. Astr. Soc.*, 59, 593-603.
- Chao, B. F., and Gilbert, F., 1980. Autoregressive estimation of complex eigenfrequencies in low-frequency seismic spectra. *Geophys. J. R. Astr. Soc.*, 63, 641-657.
- Dahlen, F. A., 1982. The effect of data windows on the estimation of free oscillation parameters. *Geophys. J. R. Astr. Soc.*, 69, 537-549.
- Dziewonski, A. M., and Anderson, D. L., 1981. Preliminary reference Earth model, *Phys. Earth planet. Inter.*, 25, 297-356.
- Hoenen, S., Schimmel, M., and Marques, M. D., 2001. Rescuing rhythms from noise: A new method of analysis. *Biological Rhythm Research*, 32, 271-284.
- Hori, S., Fukao, Y., Kumazawa, M., Furomoto, M., and Yamamoto, A., 1989. A new method of spectral analysis and its application to the Earth's free oscillations: The Sompi method. *J. geophys. Res.*, 94(B6), 7535-7553.
- Masters, G., and Gilbert, F., 1983. Attenuation in the Earth at low frequencies. *Phil. Trans. Roy. Soc. Land., Ser. A*, 308, 479-522.
- Melchior, P., 1978. *Tides of the planet Earth*. Pergamon Press.
- Nelson, W., Tong, Y. L., Lee, J. K., and Halberg, F., 1979. Methods for cosinor-rhythmometry. *Chronobiologia* 6(4), 305-324.
- Neumeyer, J., 1995. Frequency dependent atmospheric pressure correction on gravity variations by means of cross spectral analysis. *Bull. Inf. Marrées Terr.*, 122, 9212-9220.
- Park, J., Lindberg, C. R., and Thomson, D. J., 1987. Multiple-taper spectral analysis of terrestrial free oscillations: part 1. *Geophys. J. R. Astr. Soc.*, 91, 755-794.
- Lindberg, C. R., and Park, J., 1987. Multiple-taper spectral analysis of terrestrial free oscillations: part 2. *Geophys. J. R. Astr. Soc.*, 91, 795-836.
- Pollak, L. W., 1930. *Prager Geophysikalische Studien*. Heft 3 (Čechoslovak. Statistik, Reihe 12, Heft 13), Prague.
- Riedesel, M. A., Agnew, D. C., Berger, C., and Gilbert, F., 1980. Stacking for the frequencies and  $Q$ 's of  ${}_0S_0$  and  ${}_1S_0$ . *Geophys. J. R. Astr. Soc.*, 62, 457-471,
- Rosat, S., Hinderer, J., Crossley, D., and Rivera, L., 2003a. The search for the Slichter mode: comparison of noise levels of superconducting gravimeters and investigation of a stacking method. *Phys. Earth planet. Inter.*, 140, 183-202.
- Rosat, S., Hinderer, J., and Rivera, L., 2003b. First observation of  ${}_2S_1$  and study of the splitting of the football mode  ${}_0S_2$  after the June 2001 Peru earthquake of magnitude 8.4. *Geophys. Res. Lett.*, 30(21), 2111, doi:10.1029/2003GL018304.
- Santamaría, I., Pantaleón, C., and Ibañez, J., 2000. A comparative study of high-accuracy frequency estimation methods. *Mechanical Systems and Signal Processing*, 14(5), 819-834.
- Van Camp, M., 1999. Measuring seismic normal modes with the GWR C021 superconducting gravimeter. *Phys. Earth planet. Inter.*, 116, 81-92.
- Widmer-Schmidrig, R., 2003. What can superconducting gravimeters contribute to normal-mode seismology? *Bull. seism. Soc. Am.*, 93, 1370-1380.
- Zürn, W., and Rydelek, P. A., 1994. Revisiting the phasor-walkout method for detailed investigation of harmonic signals in time series. *Survey in Geophys.* (15), 409-431.
- Zürn, W., and Widmer, R., 1995. On noise reduction in vertical seismic records below 2 mHz using local barometric pressure. *Geophys. Res. Lett.*, 22(24), 3537-3540.